Polymer Chemistry

Accepted Manuscript

ROYAL SOCIETY OF CHEMISTRY

www.rsc.org/polymers

Anomalous Trade-off Effect on the Properties of Smart *ortho*-Functional Benzoxazines

Kan Zhang,*[a,b] and Hatsuo Ishida*[b]

[a]*School of Materials Science and Engineering, East China University of Science and Technology, Shanghai 200237, China.* E-mail: kxz93@case.edu

[b]*Department of Macromolecular Science and Engineering, Case Western Reserve University, Cleveland, OH, 44106, United States.* E-mail: hxi3@cwru.edu

Abstract

A series of *ortho*-difunctional benzoxazine monomers containing amide, imide and amide-imide groups have been synthesized in order to obtain basic design rules toward preparing higher performance polybenzoxazoles based on smart benzoxazine chemistry. The structures of the synthesized monomers have been confirmed by ^{1}H nuclear magnetic resonance spectroscopy (NMR) and Fourier transform infrared spectroscopy (FTIR). The polymerization behavior of benzoxazine monomers is studied by differential scanning calorimetry (DSC). The trade-off between a symmetric imide and a symmetric amide results in an asymmetric amide-imide functional monomer exhibiting broadest processing window and lowest activation energy of the *ortho*-functional benzoxazine studied. After polymerization, the thermal stability of each polybenzoxazines is studied by thermogravimertic analysis (TGA). The polymer obtained from *ortho*-(amide-imide) functional benzoxazine gives highest thermal stability, which is against the traditionally designed poly(amide-co-imide), possessing the thermal stability between polyamide and polyimide. The activation energy for benzoxazine polymerization and the degradation of polybenzoxazole are also studied by DSC and TGA, respectively. The relationship between the benzoxazine monomer structures and the thermosets properties has been discussed.

Introduction

Benzoxazine is a newly developed thermosetting resin which can be synthesized by Mannich condensation from phenol, amine, and formaldehyde.[1-3] The major advantages of polybenzoxazine include excellent mechanical and thermal properties, low water absorption, high char yield, and low surface free energy.[4–11] The most interesting and unique characteristic of this class of polymers is their extraordinarily rich molecular design flexibility that allows designing a variety of molecular structures to tailor the desired properties.

Recently discovered superior mechanical and physical properties of *ortho*-functional benzoxazines to ordinarily used para counterparts are unexpected,[12] which is counterintuitive to the commonly reported superiority of *para*-isomers over in ordinary polymers.[13-18] This anomalous properties of *ortho*-benzoxazine structure inspired us to develop two approaches by combining it with smart chemistry that leads to highly thermally stable polybenzoxazole (PBO) structure.[19,20] Cross-linked PBOs can be obtained via thermal conversion from *ortho*-amide or *ortho*-imide functional as shown in Scheme 1. The crosslinked PBOs exhibit further advantages including outstanding flexibility in the molecular design and cost effectiveness. However, both methods showed potential disadvantages during the fabrication. Although the benzoxazines have excellent solubility in normal solvents, water is released in the temperature range between 250-300 ^{o}C for the thermal conversion to form PBOs. The *ortho*-imide functional benzoxazines do not release water but instead release CO_2 at a higher temperature (400 ^{o}C). Besides, the rigid imide groups exhibit lower solubility of benzoxazines in normal organic solvents than the amide-functional benzoxazines. Furthermore, releasing a large amount of polymerization byproducts in the form of a gas within a narrow temperature range must be avoided to minimize the void formation in the resultant polymer; however, if the *ortho*-benzoxazine resin is used to prepare a

polybenzoxazines without converting it to a polybenzoxazole, production of water or CO_2 during the thermal conversion can be an advantage from flame retardation point of view.

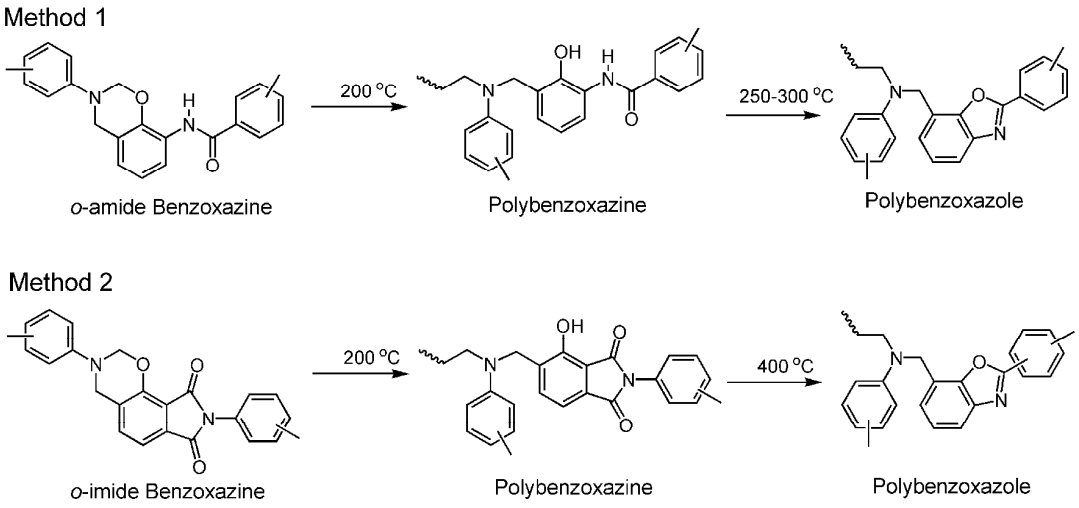

Scheme 1 Synthesis of polybenzoxazole via thermal conversion from *ortho*-amide and *ortho*-imide functional benzoxazine.

Aromatic polyimides (PIs) are widely used as matrices for advanced composites in aerospace and electronic fields due to their high thermal stability, chemical resistance, and good mechanical properties.[21] The rigidity, originating from the combination of the imide structure with an aromatic structure, results in polymers with a very high glass transition temperature (T_g).[22] However, the rigidity of PIs also causes processing difficulties. To solve the problems of processability, the backbone can be diluted with other less stable structures. Therefore, the trade-off generally exists between the thermal resistance and processability of PIs.[23] The synthesis of poly(amide-co-imide) (PAI) is one of the best methods for enhancing the processability while still maintaining excellent high performance properties. Aromatic PAI possesses balanced characteristics between polyamides and polyimides such as high thermal stability and good mechanical properties together with ease of processability.[24,25]

Inspired by the trade-off designing of PAI, we synthesized a class of polybenzoxazole precursors, *ortho*-imide, *ortho*-amide, and *ortho*-(amide-imide) difunctional benzoxazine monomers in this study (Scheme 2). An asymmetric *ortho*-(amide-imide) difunctional

benzoxazine was designed as an example trade-off monomer between symmetric *ortho*-imide and *ortho*-amide difunctional benzoxazines. More importantly, this class of benzoxazine monomers provides us with an opportunity to explore the influence of amide and imide groups as part of the *ortho*-functional groups on properties of benzoxazine monomers, polybenzoxazines, as well as the corresponding polybenzoxazoles. It is the purpose of this paper to study, systematically, the rate of oxazine polymerization and benzoxazole formation, and thermal stability of the subsequent polybenzoxazoles derived from the *ortho*-difunctional benzoxazine monomers to provide us with a fundamental understanding of the trade-off effect on benzoxazine, polybenzoxazine and polybenzoxazole properties.

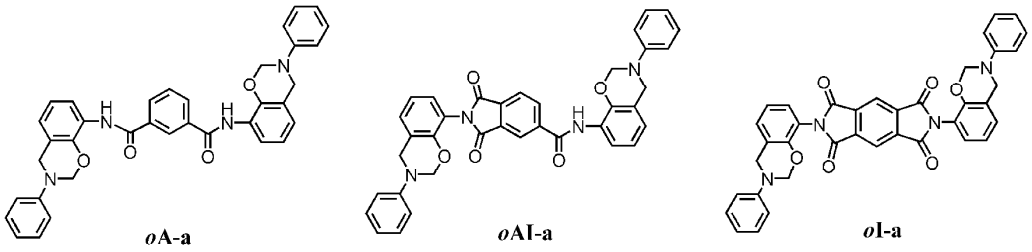

Scheme 2 Chemical structure of *ortho*-functional benzoxazines.

Experimental

Materials

o-Aminophenol (98%), trimellitic anhydride chloride (98%), pyromellitic dianhydride (97%) and paraformaldehyde (99%), were used as received from Sigma-Aldrich. Aniline was purchased from Aldrich and purified by distillation. Dimethylformamide (DMF), hexane, xylenes, 1,4-dioxane sodium bicarbonate ($NaHCO_3$) and sodium sulfate were obtained from Fisher scientific and used as received. *o*-Imide monofunctional benzoxazine and *o*-amide difunctional Benzoxazine (*o*A-a) were prepared following the method developed in our laboratory which are reported elsewhere.[19,20]

Synthesis of N-(2-hydroxyphenyl) Benzamide.

o-Aminophenol (3.00 g, 27.5 mmol) and LiCl (1.15g, 27.5 mmol) were dissolved in 25 mL NMP. The solution was cooled to 0°C, and benzoyl chloride (3.88 g, 27.5 mmol) was added dropwise with a syringe. The solution was kept at room temperature overnight. After confirming the structure of products by NMR, the reaction mixture was poured into cold water. The precipitate was filtered and afterwards dried under vacuum. Light pink crystal was obtained (yield 85%). ^{1}H NMR (DMSO-d_6), ppm: δ = 6.77-7.95 (9H, Ar), 9.51 (s, NH), 9.74 (s, OH). IR spectra (KBr, cm^{-1}): 3408 (N-H stretching), 3029 (O-H stretching), 1645 (amide Ⅰ), 747 (C=O bending).

Preparation of *o*-Amide Monofunctional Benzoxazine, N-(3-phenyl-3,4-dihydro-2*H*-benzo[e][1,3]oxazin-8-yl)benzamide.

Into a 50 mL round flask were added 20 mL of chloroform, aniline (0.44 g, 4.70 mmol), N-(2-hydroxyphenyl) benzamide (1.00 g, 4.70 mmol), and paraformaldehyde (0.23 g, 9.40 mmol). The mixture was stirred at 80°C for 24 h, and subsequently cooled to room temperature. Then, the solution was purified by washing with cold water. The chloroform solution was dried over sodium sulfate anhydrous to obtain crude product. Crude product was fractionated by the column chromatography (eluent: hexanes and ethyl acetate, volume ratio= 3:1) to obtain pure final product (yield 80%). ^{1}H NMR (DMSO-d_6), ppm: δ = 4.68 (s, Ar-CH_2-N, oxazine), 5.45 (s, O-CH_2-N, oxazine), 6.87-7.94 (13H, Ar), 9.35 (s, NH). IR spectra (KBr), cm^{-1}: 3366 (N-H stretching), 1659 (amide Ⅰ), 1238 (C-O-C asymmetric stretching), 937 (out-of-plane C-H of benzene ring to which oxazine ring is attached).

Preparation of N,2-bis(2-hydroxyphenyl)-1,3-dioxoisoindoline-5-carboxamide (Abbreviated as *o*AI).

As shown in Scheme 3, *o*AI was synthesized by reacting *o*-aminophenol with trimellitic anhydride chloride in DMF. Into a 250 mL round flask were placed trimellitic anhydride chloride (6.32 g, 0.03 mol), *o*-aminophenol (6.54 g, 0.06 mol), and 80 ml of dimethylformamide. The mixture was stirred at room temperature for 1 h, and then

refluxed at 160 °C for 6 h. After cooling to room temperature, the reaction mixture was poured into 500 mL of 2 mol/L $NaHCO_3$ aqueous solution to give a powder-like Then the precipitate was filtered and washed several times with de-ionized water. The products were dried under vacuum to obtain a yellow powder (yield 85%). ^{1}H NMR (DMSO-d_6), ppm: δ = 6.79-8.65 (11H, Ar), 9.71 (s, OH), 9.88 (s, OH), 10.01 (s, NH). IR spectra (KBr, cm^{-1}): 3364 (O-H stretching), 1779, 1709 (Imide Ⅰ), 1709, 1657 (amide Ⅰ), 1388 (imide Ⅱ,C-N stretching), 753 (C=O bending).

Preparation of Difunctional, Asymmetric *o*-(Amide-imide) Benzoxazine, 1,3-dioxo-*N*,2-bis(3-phenyl-3,4-dihydro-2*H*-benzo[*e*][1,3]oxazin-8-yl)isoindoline-5-carboxamide (Abbreviated as *o*AI-a).

Difunctional *o*-(amide-imide) benzoxazine was synthesized via a solvent method (as shown in Scheme 3). Into a 100 mL round flask were added 40 mL of mixed isomer xylenes, aniline (1.86 g, 0.02 mol), *o*AI (3.74 g, 0.01 mol), and paraformaldehyde (1.21 g, 0.04 mol). The mixture was stirred at 120 °C for 6 h. The mixture was cooled to room temperature. Then the solution was precipitated into 100 mL of hexane. Removal of solvent afforded a yellow powder (yield 95%). ^{1}H NMR (DMSO-d_6), ppm: δ = 4.68, 4.75 (s, Ar-CH_2-N, oxazine), 5.44, 5.53 (s, O-CH_2-N, oxazine), 6.54-8.57 (19H, Ar), 9.95 (s, NH). IR spectra (KBr), cm^{-1}: 1780, 1724 (imide I), 1724, 1675 (amide Ⅰ),1498 (stretching of trisubstituted benzene ring), 1380 (imide II), 1234 (C-O-C asymmetric stretching), 926 (out-of-plane C-H of benzene ring to which oxazine ring is attached).

Preparation of N_1,N_3-bis(2-hydroxyphenyl)-1,3-dioxoisoindoline (*o*I).

As shown in Scheme 3, *o*I was synthesized by reacting *o*-aminophenol with pyromellitic dianhydride in DMF. Into a 250 mL round flask were placed pyromellitic dianhydride g, 0.03 mol), *o*-aminophenol (6.54 g, 0.06 mol), and 60 ml of dimethylformamide. The mixture was stirred at room temperature for 1 h, and then refluxed for 6 h. After cooling room temperature, the reaction mixture was poured into 500 mL of cold water to give a powder-like precipitate. The products were dried under vacuum to obtain a yellow

(yield 92%). ^{1}H NMR (DMSO-d_6), ppm: δ = 6.89-8.45 (11H, Ar), 9.93 (s, OH). IR (KBr, cm^{-1}): 3327 (O-H stretching), 1773, 1703 (Imide Ⅰ), 1383 (imide Ⅱ,C-N stretching), 758 (C=O bending).

Preparation of Difunctional, Symmetric *o*-Imide Benzoxazine, 2,6-bis(3-phenyl-3,4-dihydro-2*H*-benzo[*e*][1,3]oxazin-8-yl)pyrrolo[3,4-*f*]isoindole-1,3,5,7(2*H*,6*H*)-tetraone (Abbreviated as *o*I-a).

Difunctional *o*-imide benzoxazine was synthesized via a solvent method (as shown in Scheme 3). Into a 250 mL round flask were added 100 mL of 1,4-dioxane, aniline (1.86 g, 0.02 mol), *o*I (4.00 g, 0.01 mol), and paraformaldehyde (1.21 g, 0.06 mol). The mixture was stirred at 110 ^{o}C for 24 h. The mixture was cooled to room temperature. Then the reaction mixture was poured into 500 mL of cold water to give a powder like precipitate. The product was dissolved in ethyl acetate and further purified by washing with 2 N NaOH solution and water to eliminate the residual starting materials. The purified products were dried over sodium sulfate followed by filtering and drying under vacuum to obtain a yellow powder (yield 87%). ^{1}H NMR (DMSO-d_6), ppm: δ = 4.74 (s, Ar-CH_2-N, oxazine), 5.45 (s, O-CH_2-N, oxazine), 6.49 -8.45 (19H, Ar). IR spectra (KBr), cm^{-1}: 1780, 1726 (imide I), 1487 (stretching of trisubstituted benzene ring), 1377 (imide II), 1232 (C-O-C asymmetric stretching), 924 (out-of-plane C-H of benzene ring to which oxazine is attached).

Preparation of polybenzoxazine and polybenzoxazole thermosets.

Solutions of 30% solid content of *o*A-a, *o*AI-a and *o*I-a in DMF were prepared. Then, the solution was cast over a dichlorodimethylsilane-pretreated glass plate. The films were dried in an air-circulating oven at 100 ^{o}C for 3 days to remove the solvent. The films as fixed on a glass plate were polymerized at 220 ^{o}C for 2 h to obtain polybenzoxazines. The polybenzoxazine thermosets were further treated at 300 and 400^{o}C for 1 h each, and then obtained polybenzoxazole thermosets.

Characterization. Proton nuclear magnetic resonance (^{1}H NMR) spectra were acquired a Varian Oxford AS300 at a proton frequency of 300 MHz. The average number of

transients for ^{1}H MNR measurement was 64. A relaxation time of 10 s was used for the integrated intensity determination of ^{1}H NMR spectra. Fourier transform infrared (FTIR) spectra were obtained using a Bomem Michelson MB100 FTIR spectrometer, which was equipped with a deuterated triglycine sulfate (DTGS) detector and a dry air purge unit. Coaddition of 64 scans was recorded at a resolution of 4 cm^{-1}. Transmission spectra were obtained by casting a thin film on a KBr plate for partially polymerized samples. A TA Instruments Differential Scanning Calorimeter (DSC) Model 2920 was used with a rate of 10 ^{o}C/min and a nitrogen flow rate of 60 mL/min. In the analyses to determine the activation energy of benzoxazine polymerization, the samples (2.0 ± 0.5 mg) were at different heating rates of 2, 5, 10, 15, 20 ^{o}C/min. All samples were sealed in hermetic aluminum pans with lids. Thermogravimetric analyses (TGA) were performed on a TA Instrument Q500 TGA with a heating rate of 10 ^{o}C/min in a nitrogen atmosphere at a rate of 40 mL/min. In the analyses to determine the activation energy for decomposition polybenzoxazole, the samples were scanned at different heating rates of 5, 10, 15, 20, 25 ^{o}C/min.

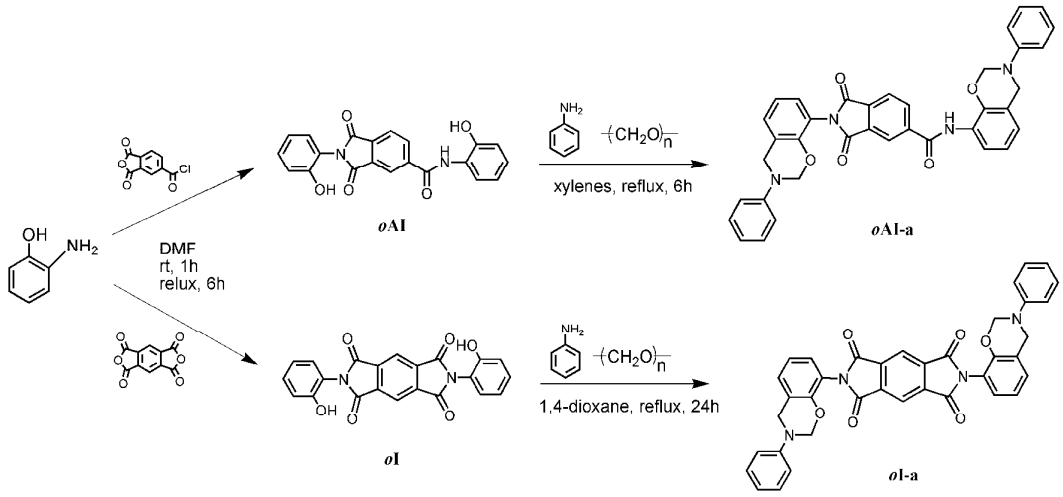

Scheme 3 Preparation of difunctional *o*-(amide-imide) and *o*-imide benzoxazine monomers.

Result and discussion

Preparation of *ortho*-Functional Benzoxazine Monomers.

An attractive class of smart benzoxazines, that are polybenzoxazole precursors, have been successfully achieved using primary amine (aniline), formaldehyde, and various phenols, including *o*-amide, *o*-(amide-imide), and *o*-imide functional phenols. In our previous work, we have synthesized difunctional *o*-amide benzoxazine (*o*A-a).[19] Here we no longer discuss the details about the preparation of *o*A-a.

Prior to this study, Huang et al. have synthesized *para*-imide difunctional benzoxazines.[26] The synthesis of *para*-imide difunctional benzoxazines required the reaction time as long as 72 hours in 1,4-dioxane at the reflux temperature. However, in the case of preparing *ortho*-functional benzoxazine, *o*I-a, the synthesis completed in just 24 hours at the reflux temperature, and a transparent solution was subsequently formed, leading to a high yield. The rigidity of imide group results in poor solubility of imide-functional diphenol in ordinary solvents, which leads to difficulty in synthesizing benzoxazine. However, the benzoxazine synthesis becomes much easier by replacing one of the imide groups into an amide group instead of two imide groups. The synthesis for *o*AI-a completed in just 6 h at 120^{o}C in xylenes. The amide-imide structure in *o*AI decreases the rigidity and increases the solubility in ordinary solvents compared with *o*I. As a result, the benzoxazine ring forming for *o*AI-a becomes much easier than *o*I-a.

Figure 1 shows the ^{1}H NMR spectra of *o*I-a and *o*AI-a. The characteristic resonances attributed to the benzoxazine structure, Ar-CH_2-N- and -O-CH_2-N- for *o*I-a, are observed 4.74 and 5.45 ppm, respectively. The corresponding resonances for *o*AI-a are observed at 4.70, 4.74 and 5.43, 5.54 ppm, respectively. Ordinarily, the characteristic benzoxazine resonance pair for Ar-CH_2-N- and -O-CH_2-N- consists of singlets with frequency separation of around 0.8-0.9 ppm.[3] However, due to the asymmetric nature of the environment of oAI-a, those singlets split into doublets. In order to qualitatively assign typical resonances of benzoxazine rings for *o*AI-a, *o*-amide and *o*-imide monofunctional benzoxazine monomers were synthesized as model compounds in this study. As depicted in Figure 2, the frequency separation of *o*-amide monofunctional benzoxazine is larger

than *o*-imide monofunctional benzoxazine. The possible reason is that the hydrogen bonding between the –NH- in amide group and the O in oxazine ring, which has stronger deshielding effect to -O-CH_2-N- than Ar-CH_2-N-. Based on ^{1}H NMR result of model compounds, it is reasonable to assign doublets of typical resonances of oxazine rings of *o*AI-a as shown in Figure 1. Moreover, the ^{1}H NMR spectra confirm the presence of group of *o*AI-a at 9.95 ppm.

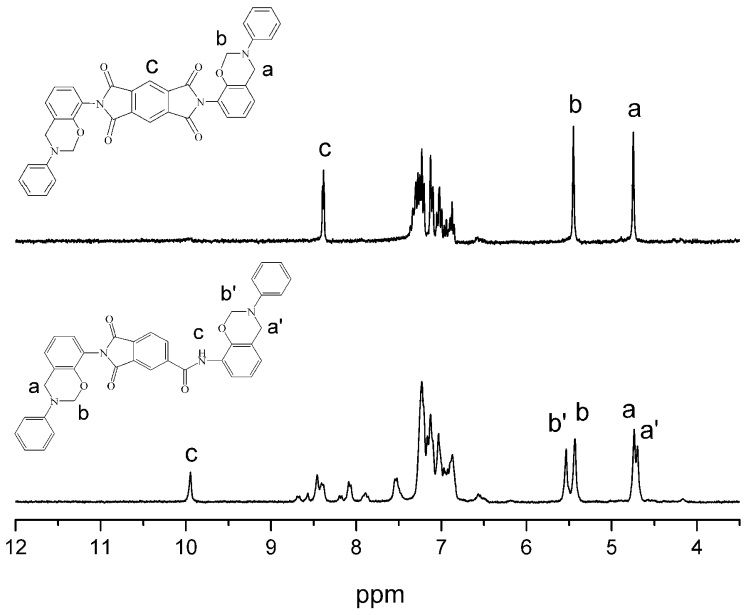

Fig. 1 ^{1}H NMR spectra of *o*I-a and *o*AI-a.

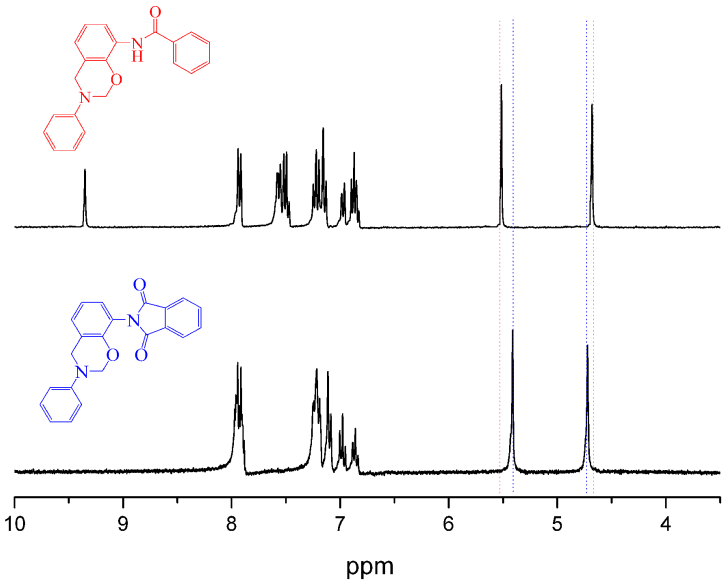

Fig. 2 ^{1}H NMR spectra of *o*-amide and *o*-imide monofunctional benzoxazines.

There are a number of infrared absorption bands, highlighted in Figure 3, that are used verify the formation of amide, imide and oxazine rings in each monomer. For example, imide is represented by the characteristic bands at 1780, 1726 cm^{-1} and 1377 cm^{-1}, and 1780, 1724, and 1380 cm^{-1} for *o*I-a and *o*AI-a, respectively. The characteristic doublets at 1780 and 1726 cm^{-1}, and 1780 and 1724 cm^{-1} are attributed to the imide C-C(=O)-C asymmetric and symmetric stretching modes, respectively.[27] The bands at 1380 and 1372 cm^{-1} are due to the axial stretching of C-N bonding.[28,29] Besides, the characteristic bands 1675 cm^{-1} (*o*AI-a) and 1664 cm^{-1} (*o*A-a) are the amide Ⅰ band. Bands for asymmetric trisubstituted benzene that appear at 1499 cm^{-1} (*o*A-a), 1498 cm^{-1} (*o*AI-a) and 1487 cm^{-1} (*o*I-a) support the incorporation of imide and amide group into benzoxazine monomers. Furthermore, the presence of the benzoxazine ring aromatic ether in the monomers is indicated by bands centered at 1226, 1234 and 1232 cm^{-1} for the *o*A-a, *o*AI-a and *o*I-a, respectively, which are due to the C-O-C asymmetric stretching modes.[30] The characteristic out-of-plane absorption modes of benzene with an attached oxazine ring are located at 924, 926 and 924 cm^{-1} for the *o*A-a, *o*AI-a and *o*I-a, respectively.[31] All the

information is consistent with the successful synthesis of the target compounds.

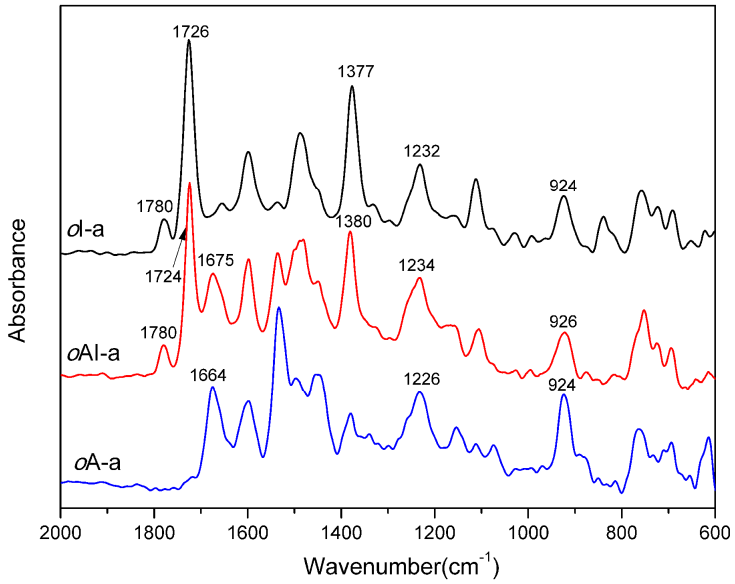

Fig. 3 FTIR spectra of benzoxazine monomers, *o*I-a, *o*AI-a, and *o*A-a.

Polymerization Behavior of Benzoxazine Monomers.

In order to better understand the ring-opening polymerization of this class of *ortho*-difunctional benzoxazines, we also studied the polymerization behavior of model compounds as depicted in Figure 4. The *o*-amide monofunctional benzoxazine is shown to polymerize at much lower temperature than ordinary benzoxazines without added initiators and/or catalysts to form amide-containing polybenzoxazine. The presence of intramolecular hydrogen bonding between an amide linkage and the adjacent oxazine ring is hypothesized to act as an incentive to stimulate the ring-opening polymerization. The *o*-imide monofunctional benzoxazine shows a higher polymerization temperature (234 ^{o}C) comparing with *o*-amide functional benzoxazine (215 ^{o}C), although it is still much lower than the phenol-aniline based benzoxazine (263 ^{o}C).[19] Unfortunately, the rigidity, originating from the combination of imide structure with an aromatic structure, results in *o*-imide monofunctional benzoxazine with a very high melting temperature.

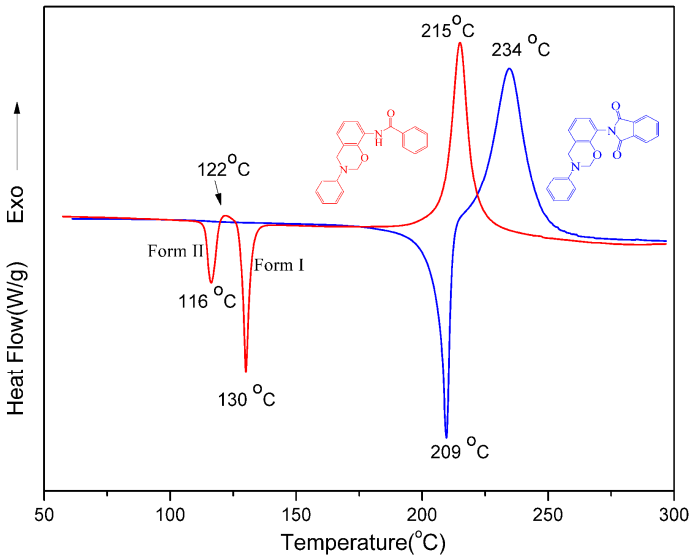

Fig. 4 DSC polymerization behavior of mono-functional benzoxazine monomers.

Interestingly, the *o*-amide functional benzoxazine shows an endothermic peak at 116 °C and a very small exothermic peak at 122 °C. Subsequently, a very sharp endothermic peak at 130 °C can be observed after the exothermic peak, which is in agreement with the phenomenon of crystal-to-crystal phase transition. During heating Form Ⅱ melts at 116 °C with ΔH_f = 28.1 J/g and thereafter crystallizes into From Ⅰ at 122 °C (ΔH_f = -12.64 J/g). The second endothermic peak at 130 °C on the DSC curves is due to the melting of Form Ⅰ. The ΔH_f for this stage is 69.4 J/g. The melting point of Form Ⅰ is higher than that of Form Ⅱ and ΔH_f (Form Ⅰ) > ΔH_f (Form Ⅱ); thus according to the Burger-Ramberger heat-of-fusion rule we conclude that the relation between these two polymorphs is monotropic.[32] The crystal of *o*-amide monofunctional benzoxazine can be recrystallized into another more stable crystal form during the melting stage. This unexpected result attracted our attention since no other benzoxazine monomers show such crystal-to-crystal phase transition. Further detailed study is needed to explain this complex phenomenon.

Figure 5 shows the polymerization profiles of these three *o*-difunctional benzoxazine monomers. The thermograms show that the maxima of the ring-opening polymerization

*o*A-a, *o*AI-a and *o*I-a centered at 209, 214 and 256 °C, respectively. The benzoxazine and *o*AI-a containing amide groups show lower polymerization temperature compared to *o*I-a which only contains imide group. The heat of polymerization values are 248, 193.4 and 92.0 J/g for *o*A-a, *o*AI-a and *o*I-a, respectively. Besides, *o*A-a and *o*AI-a exhibit the melting temperature centered at 151 and 125 °C, respectively. However, no melting temperature can be observed of *o*I-a, which determines that *o*I-a is amorphous. Moreover, *o*I-a shows a higher starting polymerization temperature (225 °C) and a narrower exothermic peak compared with *o*A-a and *o*AI-a. The rigidity, originating from the combination of two imide structure with an aromatic structure, decreases the mobility of molecules of *o*I-a during the polymerization, which likely results in the low degree of crosslinking and low heat of polymerization.

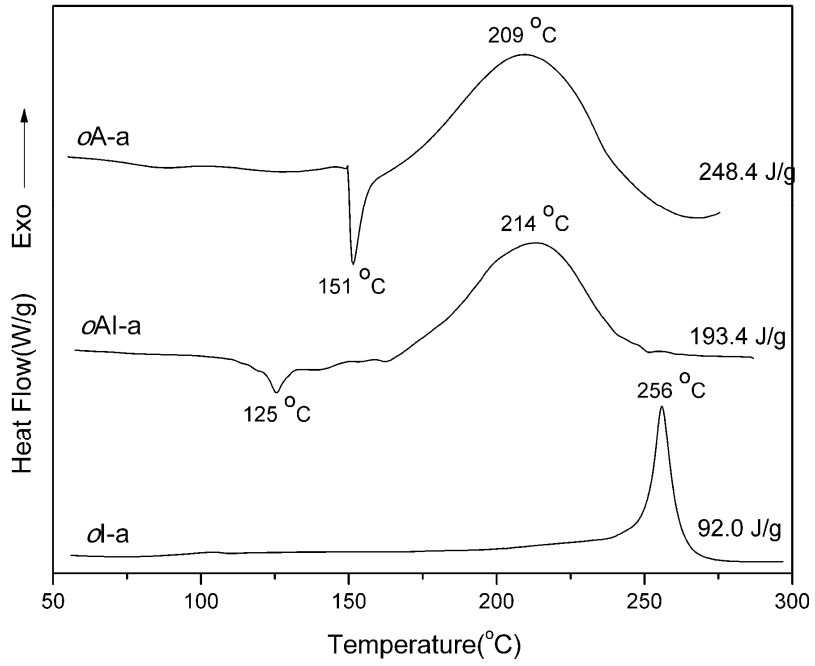

Fig. 5 DSC thermograms of *o*-difunctional benzoxazine monomers.

Figures 6 and 7 show the DSC plots of *o*AI-a and the conversion versus temperature at different heating rates. Figure 6 also shows the initial polymerization temperature (T_i) and peak temperature (T_p) at different heating rates. The figures indicate that the exothermic peak shifts to a higher temperature with the increase of heating rate as expected.

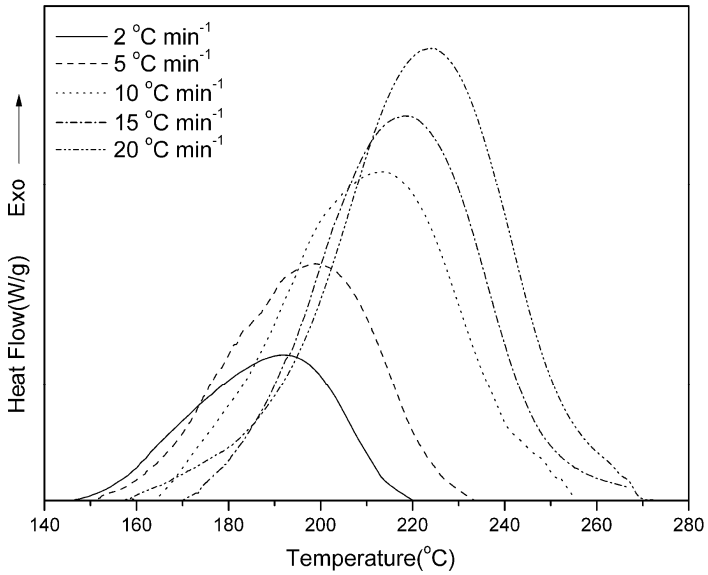

Fig. 6 DSC curves of *o*AI-a at different heating rates.

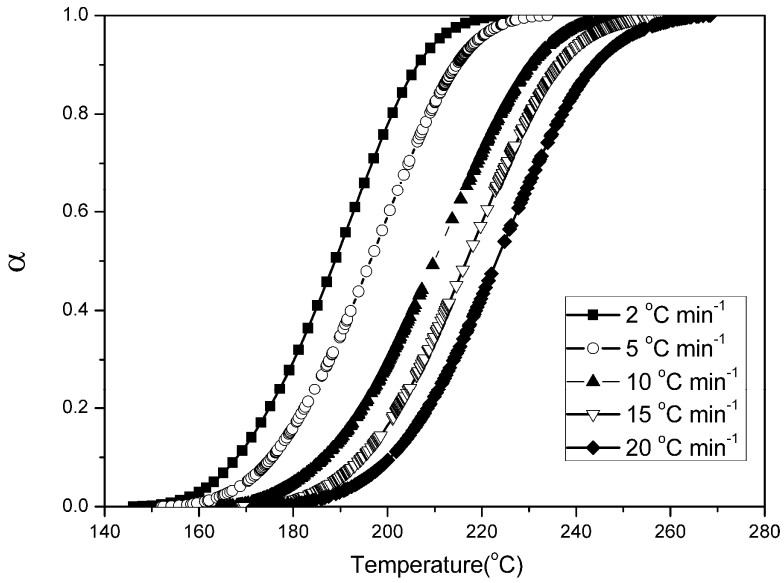

Fig. 7 Conversion vs. temperature for *o*AI-a cured at different heating rates.

The activation energy for polymerization was investigated using the well-known Kissinger and Ozawa methods.[33,34] According to the Kissinger method, the activation energy can be calculated by Eq. (1) as follows:

$$\ln(\frac{\beta}{T_p^2}) = \ln(\frac{AR}{E_a}) - \frac{E_a}{RT_P} \quad (1)$$

where β is the heating rate, A is the frequency factor, T_p is the temperature of the exothermic peak, E_a is the activation energy, and R is the gas constant. If the plot of $\ln(\beta/T_p^2)$ against $1/T_p$ is linear, E_a can be obtained from the slope of the corresponding straight line.

Another theoretical treatment, namely, the Ozawa method, can also be applied to the thermal data using Eq. (2) as follows:

$$\ln \beta = -1.052 \frac{E_a}{RT_P} + C \quad (2)$$

where C is a constant.

Figure 8 shows the plot of $\ln(\beta/T_p^2)$ and $\ln(\beta)$ against $1/T_p$ for the *o*AI-a according to the Kissinger and Ozawa methods. The E_a value was estimated to be 120.8 (Kissinger) and 122.2 (Ozawa) kJ/mol and listed in Table 1. The plots of $\ln(\beta/T_p^2)$ and $\ln(\beta)$ against $1/T_p$ for the *o*A-a and *o*I-a are given in Figure 9 and the activation values of *o*A-a and *o*I-a were calculated from the slopes of the plots and are also summarized in Table 1. The activation energy of symmetric *o*A-a was estimated to be 169.1 (Kissinger) and 167.3 (Ozawa) kJ/mol. However, the symmetric *o*I-a shows the highest activation energy (Kissinger: 247 kJ/mol; Ozawa: 250 kJ/mol). As can be seen, the asymmetric monomer *o*AI-a has the lowest activation energy among these *o*-functional benzoxazines. The results suggest that the oxazine rings of *o*AI-a are much easier to activate during the polymerization temperature compared with *o*A-a and *o*I-a.

From the DSC results, the amide-imide functional monomer *o*AI-a was found to have the broadest processing window among these three benzoxazines, suggesting clearly that it has better processability than the other two benzoxazine monomers. In addition to the processability, the activation energy study suggests synergism of having both imide and amide group on the same smart *o*-benzoxazine molecule.

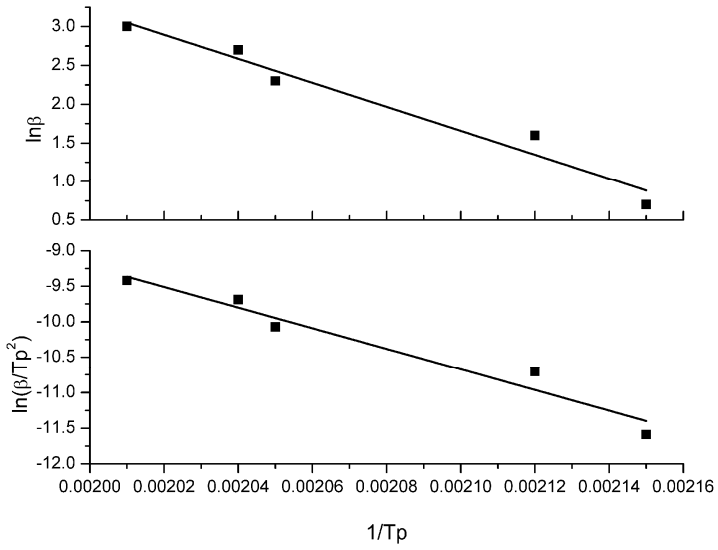

Fig. 8 Representations of Kissinger and Ozawa methods for the calculation of activation energy for *o*AI-a.

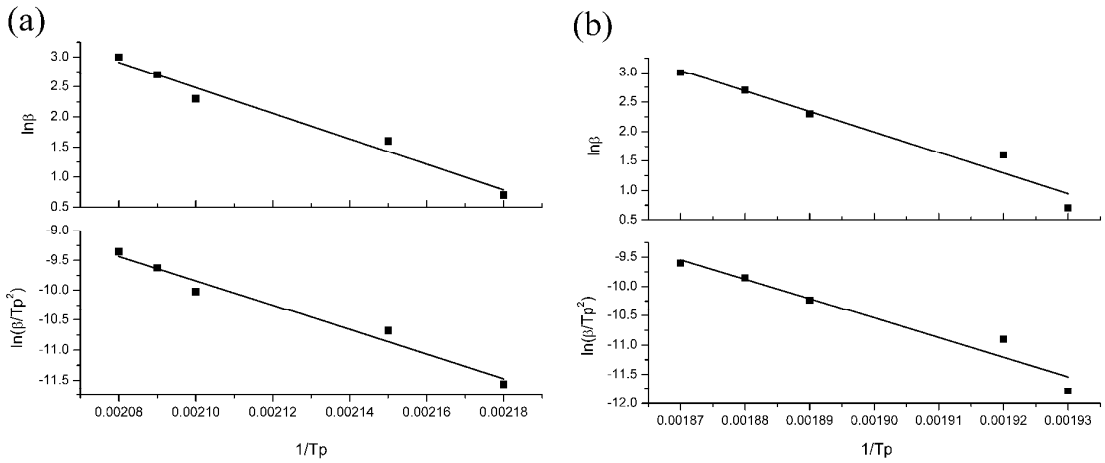

Fig. 9 Representations of Kissinger and Ozawa methods for the calculation of activation energy for (a) *o*A-a and (b) *o*I-a.

Table 1 The Activation Energy of *o*A-a, *o*AI-a and *o*I-a Obtained by Kissinger and Ozawa Methods.

Sample	Kissinger E(kJ/mol)	Ozawa E(kJ/mol)
*o*A-a	169.1	167.3
*o*AI-a	120.8	122.2
*o*I-a	247	250

Thermogravimetric Kinetic Analysis of Thermosets Derived from *o*-Difunctional Benzoxazines.

It is now found that the *ortho*-amide and *ortho*-imide functional benzoxazines are the precursors for the preparation of PBOs. The crosslinked PBOs can be obtained via thermal conversion from *ortho*-amide benzoxazines by releasing water in the range of 250-300^{o}C or *ortho*-imide benzoxazine by releasing carbon dioxide around 400 ^{o}C.[19,20] The thermal stability of polybenzoxazines derived from the three *o*-difunctional benzoxazine monomers has been studied by thermogravimetric analysis (TGA) (Figure 10) after thermal treatment at 220 ^{o}C for 2 hours. The polybenzoxazine derived from *o*A-a shows a high weight-loss stage in the range of 250-300 ^{o}C, which is due to the benzoxazole formation. The polybenzoxazine derived from *o*AI-a shows the benzoxazole formation in the range of 250-400 ^{o}C. However, poly(*o*I-a) shows a weight-loss around 300^{o}C in addition to the benzoxazole formation around 400^{o}C. The weight-loss stage around 300^{o}C can be understood by the discussion of DSC results in terms of low heat of polymerization, leading some terminal groups as defect structures, which are partially decomposed before the benzoxazole formation.

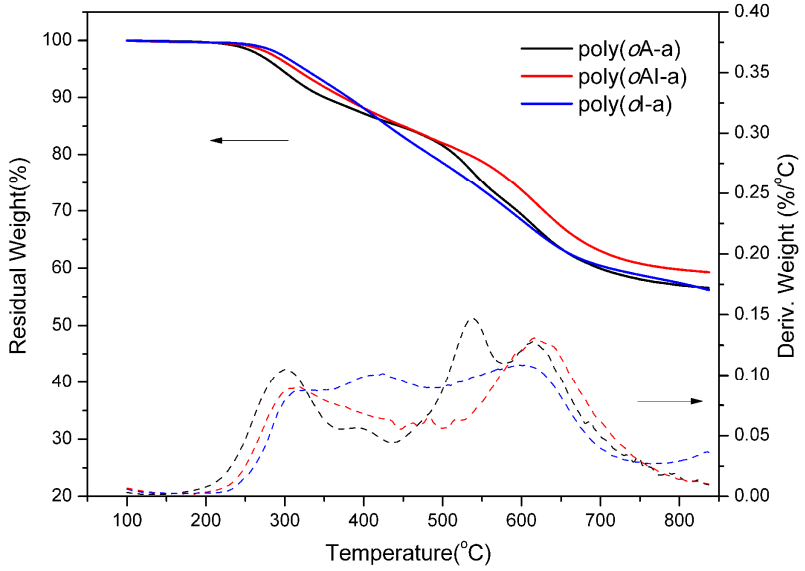

Fig. 10 Thermogravimetric analysis of *o*-difunctional benzoxazine monomers after thermal polymerization at 220 °C.

However, poly(*o*A-a) exhibits the highest weight-loss stage between 450 °C and 550 °C, which could not be observed in the thermograms of other two polymers. In order to better understand the additional degradation of poly(*o*A-a), FTIR analyses of poly(*o*A-a) after TGA measurement from room temperature to 450 °C and 550 °C at the heating rate 10 °C/min were carried out and the spectra are displayed in Figure 11. As shown in Figure 11, the characteristic bands at 1650 cm^{-1} (amide Ⅰ mode) and 1516 cm^{-1} (amide Ⅱ mode) disappeared after TGA measurement from room temperature to 450 °C, and meanwhile, the typical band of benzoxazole group at 1621 cm^{-1} which is due to C=N stretching appeared.[35,36] Besides, After TGA measurement from room temperature to 550 °C, the typical benzoxazole band at 1621 cm^{-1} still existed and even much stronger compared with other bands, implying that selective degradation of groups other than oxazole rings took place. The FTIR results suggest that the thermal conversion of *o*-hydroxypolyimide into polybenzoxazole can be mostly completed during the TGA measurement before 450 °C and the benzoxazole group is thermally stable before 550 °C. Thus, we assumed the degradation between 450 °C and 550 °C of poly(*o*A-a) in Figure 10

comes from the cross-linked segments of polybenzoxazine.

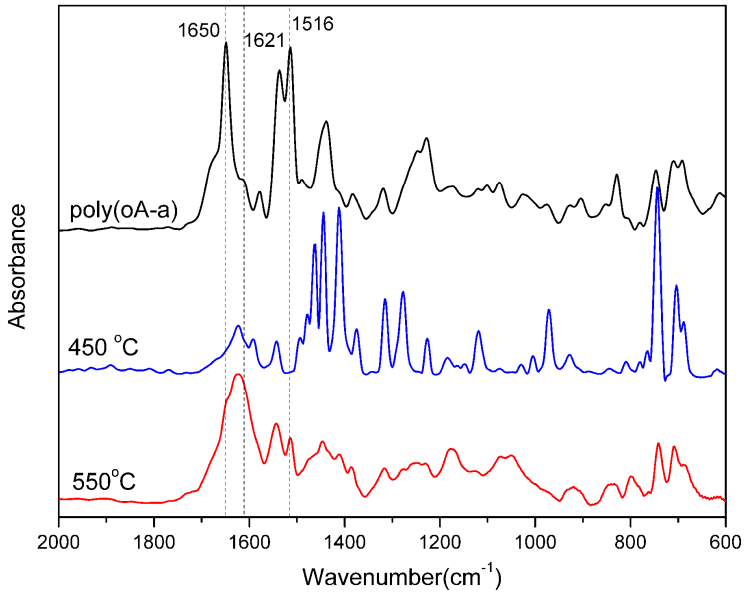

Fig. 11 FTIR spectra of poly(*o*A-a) and poly(*o*A-a) after TGA measurement from room temperature to 450 °C and 550 °C at the heating rates of 10 °C/min.

As shown in Figure 12, the heating rate was observed to have an effect on the position of the peak maximum in the derivative data for these three polybenzoxazines and with increasing heating rate the peak maximum is raised to a higher temperature regime. Hamerton et al. reported the heating rate has less influence on the nature of the initial degradation (between 200 and 300 °C, which is due to the defect structures[37,38]) for poly(BA-a) (BA-a is formed from bisphenol A and aniline).[39] However, the heating rate shows great influence on the initial benzoxazole formation for poly(*o*A-a) and poly(*o*AI-a), but less influence on poly(*o*I-a), which further implies the existence of the defect structures in poly(*o*I-a) due to its rigidity. Since the benzoxazole formation overlapped with a partial degradation of defect structures, it is very difficult to accurately and quantitatively analyze the kinetics of benzoxazole formation. However, all three polybenzoxazines show the degradation around 620°C, and the peak maximum here is raised to a higher temperature regime with increasing heating rate, which is due to the

degradation of the final cross-linked polybenzoxazole networks.

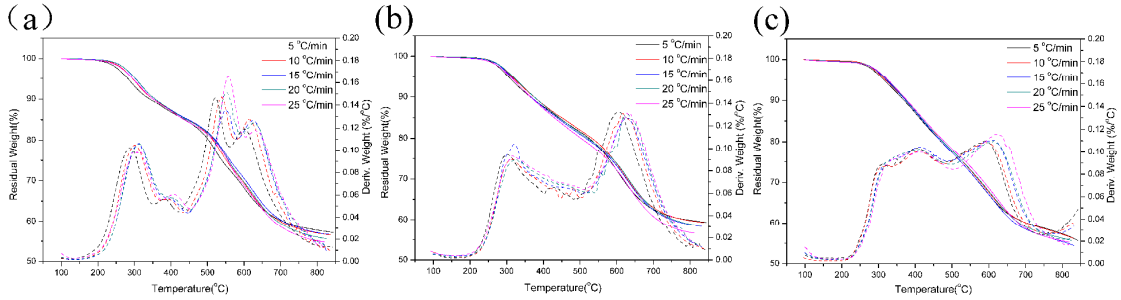

Fig. 12 TGA data of (a) poly(*o*A-a), (b) poly(*o*AI-a) and (c) poly(*o*I-a) in nitrogen as a function of heating rate.

In order to better understand the degradation kinetics of these smart thermosets, the activation energy of the degradation was evaluated using the method proposed by Kissinger.[33] It is possible to evaluate the activation energy from a plot of the following equation:

$$\ln(\frac{\beta}{T_{\mathrm{m}}^2}) = \ln(\frac{AR}{E_d}) - \frac{E_d}{RT_m}$$

where β is the heating rate, A is the frequency factor, T_m is the maximum rate decomposition temperature, E_d is the activation energy, and R is the gas constant. If the plot of $\ln(\beta/T_m^2)$ against $1/T_m$ is linear, E_d can be obtained from the slope of the corresponding straight line. Herein, we treat the T_m as the most rapidly decomposing temperature around 620 °C for each polybenzoxazole.

Figure 13 shows the plot of $\ln(\beta/T_m^2)$ against $1/T_m$ for each polybenzoxazole according to the Kissinger method. The calculated activation energies for thermal decomposition are 340, 359 and 240 kJ/mol for poly(*o*A-a), poly(*o*AI-a) and poly(*o*I-a), respectively. As can be seen, poly(*o*AI-a) has the highest activation energy for thermal decomposition among these thermosets.

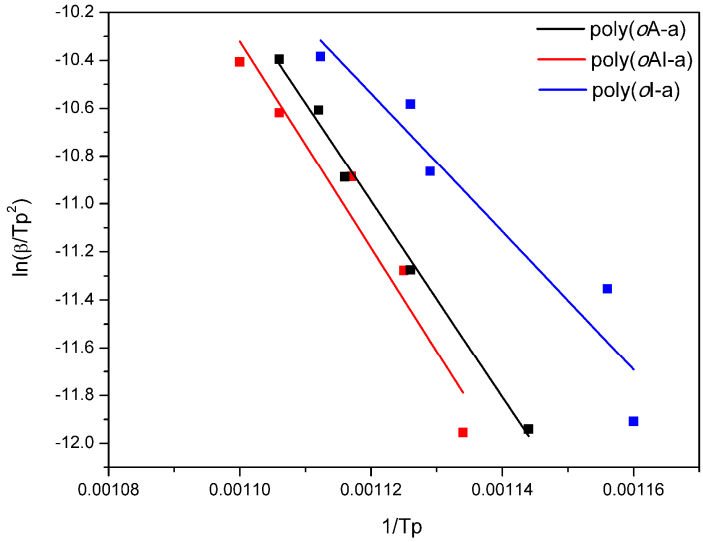

Fig. 13 Representations of Kissinger method for the calculation of decomposing activation energy for poly(*o*A-a), poly(*o*AI-a) and poly(*o*I-a).

Thermal Properties of Polybenzoxazoles derived from *o*-difunctional benzoxazines.

The thermal stability of polybenzoxazoles derived from *o*-difunctional benzoxazines has been studied by TGA as shown in Figure 14. The temperature for the degradation of these three polymers can be observed by the derivative weight loss curves. The 5% and 10% weight loss temperatures (T_{d5} and T_{d10}) for poly(*o*AI-a) are 536 ^{o}C and 589 ^{o}C, respectively. The char yield for poly(*o*AI-a) is as high as 71%, which is higher than poly(*o*A-a) (66 %) and poly(*o*I-a) (69%). The thermal property data of polybenzoxazoles are summarized in Table 2. The polybenzoxazole derived from *ortho*-(amide-imide) functional benzoxazine shows the highest thermal stability among the compounds studied.

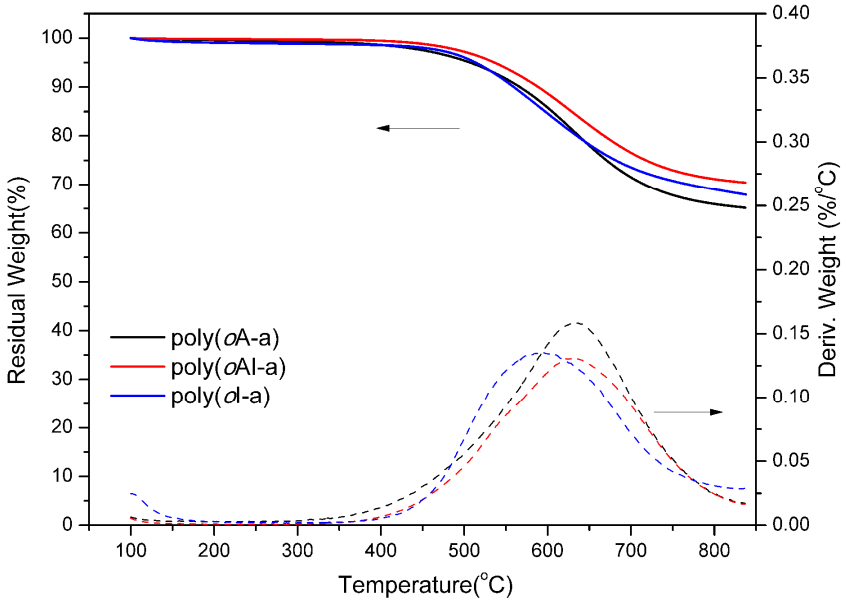

Fig. 14 Thermogravimetric analysis of poly(*o*AI-a) and poly(*o*AI-ddm) after thermal treatment at 400 °C.

Table 2. Thermal Properties of poly(*o*AI-a) and poly(*o*AI-ddm).

Sample	T_{d5} (°C)	T_{d10} (°C)	Yc (wt.%)
poly(*o*A-a)	507	567	66
poly(*o*AI-a)	536	589	71
poly(*o*I-a)	513	559	69

Conclusions

Three polybenzoxazole precursors, *o*-difunctional benzoxazines, were successfully synthesized in this study in aim to understand the effect of different *o*-functional benzoxazine structures on the thermal properties, such as polymerization exotherm temperature, monomer polymerization kinetics, benzoxazole formation and degradation

behaviors under inert atmosphere. Unexpectedly, it was found that the trade-off *ortho*-(amide-imide) difunctional benzoxazine has the broadest processing window and the corresponding polybenzoxazine has the highest thermal stability, which is against to the traditional designed poly(amide-co-imde), possessing the processability and thermal stability between polyamide and polyimide. Additionally, the polymerizing activation energy value of *ortho*-(amide-imide) functional benzoxazine was estimated to be as low as 120.8 (Kissinger) and 122.2 (Ozawa) kJ/mol, and the calculated activation energy for thermal decomposition of its corresponding polybenzoxazole was as high as 359 kJ/mol.

Acknowledgements

K. Zhang gratefully acknowledges the partial financial support of Chinese Scholarship Council (CSC) Program.

References

1 F. Holly and A. C. Cope, *J. Am. Chem. Soc.,* 1944, **66**, 1875-1879.

2 X. Ning and H. Ishida, *J. Polym. Sci., Part A: Polym. Chem.*, 1994, **32**, 1121-1129

3 H. Ishida, in *Handbook of Benzoxazine Resins*, ed. H. Ishida and T. Aaga, Elsevier, Amsterdam, 2011, pp 3-81.

4 H. Ishida and D. J. Allen, *Poymer,* 1996, **37**, 4487-4495.

5 H. Ishida and H. Y. Low, *Macromolecules,* 1977, **30**, 1099-1106.

6 H. J. Kim, Z. Brunovska and H. Ishida, *J. Appl. Polym. Sci.,* 1999, **73**, 857-862.

7 H. J. Kim, Z. Brunovska and H. Ishida, *Polymer,* 1999, **40**, 1815-1822.

8 K. Zhang, Q. X. Zhuang, X. Y. Liu, G. Yang, R. L. Cai and Z. W. Han, *Macromolecules,* 2013, **46**, 2696-2704.

9 K. Zhang, J. Liu and H. Ishida, *RSC. Adv*., 2014, **4**, 62550-62556.

10 Y. Yagci, B. Kiskan and N. N. Ghosh, *J. Polym. Sci., Part A: Polym. Chem.,* 2008, **47**, 5565-5576.

11 L. Qu and Z. Xin, *Langmuir,* 2011, **27**, 8365-8370.

12 J. Liu and H. Ishida, *Macromolecules,* 2014, **47**, 5682-5690.

13 M. K. Ghosh and K. L. Mittal, *Polyimides: Fundamentals and Applications*, Marcel Dekker, New York, 1996.

14 X. Q. Liu, M. Jikei and M. Kakimoto, *Macromolecules,* 2001, **34**, 3146−3154.

15 T. J. Dingemans, E. Mendes, J. J. Hinkley, E. S. Weiser and T. L. StClair, *Macromolecules,* 2008, **41**, 2474−2483.

16 C. J. Campo, T. Anastasiou and K. E. Ulrich, *Polym. Bull.,* 1999, **42**, 61−68.

17 J. Reams and D. Boyles, *J. Appl. Polym. Sci.,* 2011, **121**, 756−763.

18 C. Yang, Q. Wang, H. L. Xie, G. Q. Zhong and H. L. Zhang, *Liq. Cryst.,* 2010, **37**, 1339−1346.

19 T. Agag, J. Liu, R. Graf, H. W. Spiess and H. Ishida, *Macromolecules,* 2012, **45**, 8991-8997.

20 K. Zhang, J. Liu and H. Ishida, *Macromolecules,* 2014, **47**, 8674-8681.

21 P. Vandezande, L. E. M. Gever and I. F. J. Vankelecom, *Chem. Soc. Rev.*, 2008, **37**, 365-405.

22 A. J. Kirby, Polyimide: Materials Processing and Applications, *Oxford: Pergamon Press*, 1992, vol. 5, pp. 158.

23 P. E. Cassidy and N. C. Fawcett, in Encyclopedia of Polymer Science and Technology, ed. H. F. Mark and A. Standen, *New York: John Wiley & Sons*, 1979, vol. 118, pp. 704-719.

24 Imai, Y, *in Polyimide: Fundamentals and Applications*, ed. M. K. Ghosh and K. L. Mittal, Marcel Dekker, New York, 1996, pp 49-70.

25 I. Bacosca, E. Hamciuc, M. Bruma and M. Ignat, *React. Funct. Polym.,* 2011, **71**, 905-915.

26 Y. Gao, F. Huang, Q. Yuan, Y. Zhou and L. Du, *High. Perform. Polym.,* 2013, **25**, 677-684.

27 K. P. Pramoda, S. L. Liu and T. S. Chung, *Macromol. Mater. Eng.,* 2002, **287**, 931-937.

28 H. Ishida, S.T. Wellinghoff, E. Baer and J. L. Koenig, *Macromolecules*, 1980, **13**, 826-834.

29 B. T. Low, Y. Xiao, T. S. Chung and Y. Liu, *Macromolecules,* 2008, **41**, 1297-1309.

30 T. Agag and T. Takeichi, *Macromolecules,* 2003, **36**, 6010-6017.

31 J. Dunkers and H. Ishida, *Spectrochim. Acta.,* 1995, **51 A**, 1061-1074.

32 A. Burger and R. Ramberger, *Microchim. Acta,* 1979, **2**, 259-271.

33 H. E. Kissinger, *Anal. Chem.,* 1957, **29**, 1702-1706.

34 T. J. Ozawa, *Thermal. Anal.,* 1970, **2**, 301-324.

35 D. Likhatchev, C. Gutierre-Wing, I. Kardash and R. Vera-Graziano, *J. Appl. Polym. Sci.,* 1996, **59**, 725-735.

36 P. Bassignans, C. Cogrossi and M. Gandino, *Spectrochim. Acta.,* 1963, **19**, 1885-1897.

37 H. Y. Low and H. Ishida, *J. Polym. Sci., Part A: Polym. Phys.,* 1998, **36**, 1935-1946.

38 H. Y. Low and H. Ishida, *Polymer,* 1999, **40**, 4365-4376.

39 I. Hamerton, S. Thompson, B. J. Howlin and C. A. Stone, *Macromolecules,* 2013, **46**, 7605-7615.